Electron Delocalization in Atomic and Molecular Systems

Petar M. Mitrasinovic*

Department of Chemistry and Biochemistry, The Florida State University, Tallahassee, Florida 32306-4390

Received: April 20, 2002; In Final Form: August 8, 2002

Electron delocalization in atomic and molecular systems in terms of the single particle delocalization index (Fulton, R. L. *J. Phys. Chem.* **1993**, *97*, 7516) is analyzed. The single particle delocalization index is a quantitative measure of the degree of sharing of an electron between two disjoint regions in a many electron system. The overall focus of this paper is the determination of spatial regions in atoms from which electrons are greatly delocalized. The delocalization indices from spherical volumes of various radii centered on the nucleus of interest to the volumes outside those regions show remarkably well-defined shell structure. The delocalization shell structure exhibits spatial regions in atoms, determined by the intershell minima, in which electrons are essentially localized. The delocalization shell structure of the electrons is apparent in all the atoms in the last column of the periodic table of the elements (Ne $^1S_0$, Ar $^1S_0$, Kr $^1S_0$, Xe $^1S_0$, and Rn $^1S_0$), even in heavy atoms such as gold (Au $^2S_{1/2}$) where by traditional methods the shell structure is not clear. The delocalization shell structure of the electrons in zinc (Zn $^1S_0$) is also displayed because the expected shell structure, corresponding to principal quantum number $n = 4$, was not firmly established by previous indicators until atomic number 32 was reached. The values of distinct maxima of the delocalization indices, corresponding to regions within inner shells, are quite remarkable and related to the number of the electrons in each shell quantitatively. The physical meaning of these values is that the sharing of the core electrons in each shell does not extend to outer regions. The core shell structures in carbon (C $^3P_0$) and silicon (Si $^3P_0$) are mimicked by means of a set of the simulated natural orbitals (based on Slater's rules) used to construct the delocaliztaion index as a function of the distance from the nucleus. The separation of the contributions of definite angular momenta to the delocalization index for Ne $^1S_0$, Ar $^1S_0$, Zn $^1S_0$, Xe $^1S_0$, and Au $^2S_{1/2}$ is carried out. Interference effects between these contributions are substantially restricted to the valence region. The values of the maxima of the contributions of definite angular momenta to the delocalization index are in agreement with the number of the s-, p-, d-, and f-electrons in each shell quantitatively. This is in agreement with well-known fact that the valence electrons only tend to be chemically active. The delocalization shell structures around the heavy atoms in the molecules LiH, H_2O, CH_4, SiH_4, NH_3, and PH_3 are also displayed and compared to those around the single atoms Li $^2S_{1/2}$, O $^3P_2$, C $^3P_0$, Si $^3P_0$, N $^4S_{3/2}$, and P $^4S_{3/2}$. The delocalization of the core electrons remains essentially unchanged by incorporating the atoms into the molecules. The modifications of electron delocalization in the valence region are clear, and the chemically active regions in the molecules are nicely visible.

I. Introduction

One of the beauties of the invariant description of electron behavior developed by R. L. Fulton[1] is that many contacts can be made with more traditional (and noninvariant) modes of interpreting electron behavior. There have been numerous attempts to relate the noninvariant descriptions of electron behavior to such notions as atomic shells, lone electron pairs, pi-electron systems, etc. Existing descriptions of electron behavior include the electron structures of G. N. Lewis,[2,3] the concept of bond number advocated by L. C. Pauling,[4] the concept of bond order introduced by C. A. Coulson,[5] and the various elaborations of these which have appeared in the literature.[6] Although useful, there are well-known problems associated with many current definitions of bond orders and indices in terms of their dependencies on the particular set of orbitals and arbitrary localization procedures. As such they can have no physical meaning. The more detailed description of the behavior of electrons provided by the "Fermi" hole[7−11] is independent of the particular set of orbitals used to construct the wave function, but the "Fermi" holes are derived from the two-particle distribution function. However, Fermi holes have a semblance of localized orbitals in both atoms[8] and molecules.[12] The unitary transformations, which generate equivalent localized orbitals of the canonical orbitals of Hartree−Fock theory keeping the many particle wave function unchanged, provide a link between the molecular-orbital theory and an intuitive picture of the electronic structure.[13,14] The molecular orbitals still allow us to think in terms of the behavior of single electrons.

D. Becke and K. E. Edgecombe[15] have noted that physically meaningful descriptions of electron behavior must be sought in the density matrix (or related functions) and not in the orbitals. Wave functions (or more generally density matrixes) are therefore indispensable for the interpretation of electron behavior. Bader and co-workers[16] recognized an alternative orbital-independent description of electron localization based on the

* To whom correspondence should be addressed. E-mail: pmitrasi68@yahoo.com.

10.1021/jp025980j CCC: $22.00
Published on Web 10/24/2002

electronic density. J. G. Ángyán and M. Loos[17] have given a definition of the bond order that is consistent with the sharing index,[1] though the theoretical reasoning behind it is completely different. Fradera et al.[18] have introduced nonarbitrary the delocalization index which is equivalent to Fulton's delocalization index[1] at the Hartree−Fock level of approximation, but the delocalization index[18] is derived from the second-order density matrix. Hunter's model[19] for a single electron has a few problems associated with both the contributions to the kinetic energy of a single particle and interpreting the square root of the "spin" traced density of an electron needed to obtain the one-electron potential as a function of distance from the nucleus. The concepts of sharing of electrons[1] used in this paper are rooted in the first order density matrix. They are invariant under transformations of the orbitals in terms of which the wave function is constructed and independent of the sufficiently complete basis set.

Various authors in the literature have discussed the problems of displaying shell structure in atomic systems. The electron density distribution described by A. M. Simas et al.,[20] a well-known indicator of shell structure in light elements, failed to show more than five shells, even in the heaviest atoms. The Laplacian of the electron density proposed by R. F. W. Bader et al.[16,21] has also failed to display more than five shells (R. P. Sagar et al.[22] and Z. Shi and R. J. Boyd[23]). The one-electron potential defined by G. Hunter[19] has been used by R. P. Sagar et al.[24] to reveal up to seven shells in heavy atoms. However, the shell structure, corresponding to principal quantum number $n = 4$, was not clearly established until atomic number 32 was reached. As an orbital independent measure of the electron localization, the electron localization function (ELF) developed by A. D. Becke and K. E. Edgecombe[15] is based on the Hartree−Fock pair probability. The number of exhibited shells in the noble gas atoms Ne through Rn and in zinc by ELF was correct. The ELF was defined on the basis of the ratio between the function D_σ (inhomogeneous electron gas) and the function D_σ^0 (a uniform electron gas or electron gas reference with spin density equal to the local value of $\rho_\sigma(r)$) by performing the Taylor expansion of the spherically averaged conditional pair probability. The asymptotic ($r \rightarrow \infty$) behavior of ELF deserves our attention. All plots exhibited vanishing ELF in asymptotic regions except that for the Zn atom showing ELF of unity.[15] Y. Tal and R. F. W. Bader[25] have shown that the function D_σ vanishes asymptotically in finite systems. The physics underlying ELF is not clear with respect to both the definition of ELF and work by Y. Tal and R. F. W. Bader.[25] It was recognized by R. F. W. Bader and co-workers[21] that the numbers, locations, and relative sizes of the bonded and nonbonded charge concentrations in the valence shell of an atom in a molecule determined by the Laplacian of the charge density are in good agreement with the corresponding properties of the bonded and nonbonded localized electron pairs in valence-shell electron-pair repulsion (VSEPR) theory introduced by Gillespie.[26] The electron localization function mentioned above was supposed to be "a faithful visualization of VSEPR theory in action".[15]

In this study, Fulton's delocalization index[1] is used to examine the shell structure of the electrons in many electron systems. The scenario for constructing the measure is as follows. As a quantitative measure of electron delocalization from one region to another in atoms and molecules, the delocalization index is constructed by integrating one point of the point-point sharing index over one region and another over another region. The point-point sharing index, denoted by $I(\zeta,\zeta')$, is a quantitative measure of the degree to which an electron, as a wave, is shared between two spatial points in systems containing many electrons. The point-point sharing index is derived from the matrix element of a sharing amplitude, $\langle\zeta;\zeta'\rangle$. The sharing amplitude is defined as the square root of the first-order density matrix. The single particle sharing amplitude is the closest one can get to a wave function for a single electron in a many electron system.[1]

The plan of this paper is as follows. In part II, a brief description of the theoretical reasoning behind the delocalization index is presented. The primary intention of this part is to emphasize a natural interpretation of the delocalization of an electron between two disjoint regions in a many electron system. In part III, the inner shell structures of C and Si are mimicked by a set of the simulated natural orbitals. The delocalization shell structures in the noble gas atoms Ne through Rn and zinc are exhibited by using the delocalization index in part IV. The decomposition of the delocalization index into components of definite angular momenta for Ne, Ar, Zn, Xe, and Au is carried out in part V. In part VI, the delocalization of an electron in the heavy atoms in the molecules LiH, H_2O, CH_4, SiH_4, NH_3, and PH_3 is discussed and qualitatively compared to that in the single atoms Li, O, C, Si, N, and P.

II. Delocalization Index

Classical Sharing Index. Consider a quantity, which is distributed between two centers (positions) 1 and 2. Let the fraction of the quantity on center a be f_a: $a = 1, 2$. The sum rule obeyed by the fractions is

$$f_1 + f_2 = 1$$

A measure of the evenness of the distribution of the quantity between the centers a and b, called a sharing index, is

$$I_{ab} \equiv f_a \cdot f_b$$

I_{11} and I_{22} are self-sharing indices. $I_{12} = I_{21}$ is the inter-center sharing index. $I_{12} = I_{21} = {}^1/_4 = 0.25$ indicates that the quantity is evenly distributed between the centers.

Quantal Sharing Index. If the spatial variables r and the spin variable σ are denoted by a single index ζ, the first-order density matrix $\rho(\zeta,\zeta')$ can be found from the many electron wave function Ψ in an N electron system by integration over $N - 1$ variables:

$$\rho(\zeta,\zeta') \equiv \int d\zeta^{N-1}\, \Psi(\zeta,\zeta^{N-1})\Psi^*(\zeta',\zeta^{N-1})$$

The positive semidefinite square root of the first-order density matrix, denoted by $\rho^{1/2}(\zeta,\zeta')$, has the following property

$$\int d\zeta''\rho^{1/2}(\zeta,\zeta'')\rho^{1/2}(\zeta'',\zeta') = \rho(\zeta,\zeta')$$

The matrix element of a sharing amplitude[1] $\langle\zeta;\zeta'\rangle$ is defined as

$$\langle\zeta;\zeta'\rangle = N^{1/2}\rho^{1/2}(\zeta,\zeta')$$

The point−point sharing index[1] is defined by

$$I(\zeta,\zeta') \equiv |\langle\zeta;\zeta'\rangle|^2$$

The product $d\zeta I(\zeta,\zeta')d\zeta'$ represents a quantitative measure of the degree to which an electron as a wave is shared between a volume $d\zeta$ about ζ and a volume $d\zeta'$ about ζ'.

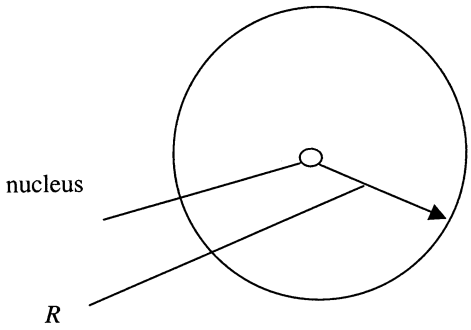

Figure 1. Spherical volume centered on the nucleus of interest.

Volume−Volume Sharing Index. The volume−point sharing index can be observed as being the microscopic valence structure of an atom in a molecule. The definition of this index is

$$I_A(\zeta) \equiv \int_A d\zeta' I(\zeta;\zeta')$$

where the integral is over a volume around an atom A. The volume−point sharing index gives a quantitative measure of the degree of sharing of a single electron between the volume associated with an atom and a point. The subsequent integral of $I_A(\zeta)$ over the volume *B*,

$$I_{AB} = \int_B d\zeta\, I_A(\zeta)$$

gives the volume−volume sharing index I_{AB}. The volume−volume sharing index, for A ≠ B, represents a quantitative measure of the degree of sharing of an electron between the volumes associated with atoms A and B. The index is also called the delocalization index. While the definition of the volume−volume sharing index is general for any method of defining atomic volumes, the actual results depend on the method used to define the atomic volumes.

III. Electron Delocalization in Atomic Systems for Simulated Natural Orbitals

The delocalization of an electron in an atom is investigated between two specially chosen volumes of varying extents: an inner spherical volume of radius *R* centered on the nucleus, and the remaining volume (Figure 1). The degree of sharing of an electron between the two volumes is determined by integrating one point of the point-point sharing index over the first and another over the second volume.

The atomic overlap integral[27] of the natural spin−orbitals $\varphi_m(\zeta)$ and $\varphi_n(\zeta)$ over volume A is denoted by

$$(\varphi_m,\varphi_n)_A^{\,s} \equiv \int_A d\zeta \varphi_m^*(\zeta)\varphi_n(\zeta)$$

where the inclusion of spin variable in the integration is indicated by the superscript s. On the basis of the spectral representation of the density matrix (normalized to 1),[28] the point−point sharing index $I(\zeta,\zeta')$, in terms of the eigenfunctions and eigenvalues of the first-order density matrix, is given by

$$I(\zeta;\zeta') = N\sum_{m,n} \varphi_m(\zeta)\rho_m^{1/2}\,\varphi_m^*(\zeta')\varphi_n(\zeta')\rho_n^{1/2}\,\varphi_n^*(\zeta)$$

and the volume−volume sharing index is given as

$$I_{AB} = N\sum_{m,n} \rho_m^{1/2}(\varphi_m,\varphi_n)_A^{\,s}\rho_n^{1/2}(\varphi_n,\varphi_m)_B^{\,s}$$

This form of I_{AB} is convenient for applications and used below to construct the delocalization index as a function of *R*.

The structure of the core shells in carbon and silicon is displayed using some orbitals which simulate the natural core orbitals of atoms. The shells of the core region are of particular interest because electrons in each shell of the core are not expected to share greatly in outer regions.

Let us assume that the natural orbitals used to mimic the core shell structure are simulated by the following set of orbitals

$$(1s):\ \left(\frac{\zeta_{1s}^{\,3}}{\pi}\right)^{1/2} e^{-\zeta_{1s}r}$$

$$(2s):\ \left(\frac{3\zeta_{2s}^{\,5}}{8\pi}\right)^{1/2} \frac{\left[1-\frac{1}{6}(2\zeta_{1s}+\zeta_{2s})r\right]}{(4\zeta_{1s}^{\,2}-2\zeta_{1s}\zeta_{2s}+\zeta_{2s}^{\,2})^{1/2}} e^{-\zeta_{2s}r/2}$$

$$(2p_z):\ \frac{1}{4\sqrt{2}}\left(\frac{\zeta_{2p}^{\,5}}{\pi}\right)^{1/2} r e^{-\zeta_{2p}r/2}\cos\theta$$

$$(2p_x):\ \frac{1}{4\sqrt{2}}\left(\frac{\zeta_{2p}^{\,5}}{\pi}\right)^{1/2} r e^{-\zeta_{2p}r/2}\sin\theta\cos\phi$$

$$(2p_y):\ \frac{1}{4\sqrt{2}}\left(\frac{\zeta_{2p}^{\,5}}{\pi}\right)^{1/2} r e^{-\zeta_{2p}r/2}\sin\theta\sin\phi$$

All the orbitals, when integrated over all space, are normalized to 1. The 1s and 2s orbitals are orthogonal to one another because the orbitals are supposed to simulate the eigenfunctions of the first-order density matrix. The $2p_{x,y,z}$ orbitals are also orthogonal to both one another and the s orbitals. The corresponding exponents are based on Slater's rules.[29] The exponents are $\zeta_{1s} = 5.7$ for carbon and $\zeta_{1s} = 13.7$, $\zeta_{2s} = \zeta_{2p} = 9.85$ for silicon. Due to the unreliability of Slater's rules for $n \geq 4$, only sample elements in the first three rows of the periodic table have been considered.

To address the question of the amount of total sharing of an electron from an inner spherical region to outside across a spherical surface of radius *R*, the integration process is carried out over the two volumes, that is, over the first volume between 0 and *R* and over the second between *R* and + ∞. For the second-row elements having 2 electrons in the cores, the 1s orbital is only used in the formula given below. For all the atoms having 10 electrons in the cores, e.g., for the third-row elements, the formula used to construct the delocalization index, as a function of *R*, is as follows.

$$\begin{aligned} I(R) = 2\Big\{ &\int_0^R r^2\,dr\int_0^\pi \sin\theta\,d\theta\int_0^{2\pi} d\phi(1s)^2 \times \\ &\int_R^\infty r^2\,dr\int_0^\pi \sin\theta\,d\theta\int_0^{2\pi} d\phi\,(1s)^2 + \\ &+\int_0^R r^2\,dr\int_0^\pi \sin\theta\,d\theta\int_0^{2\pi} d\phi(2s)^2 \times \\ &\int_R^\infty r^2\,dr\int_0^\pi \sin\theta\,d\theta\int_0^{2\pi} d\phi(2s)^2 + \\ &+3\int_0^R r^2\,dr\int_0^\pi \sin\theta\,d\theta\int_0^{2\pi} d\phi(2p)^2 \times \\ &\int_R^\infty r^2\,dr\int_0^\pi \sin\theta\,d\theta\int_0^{2\pi} d\phi(2p)^2 + \\ &+2\int_0^R r^2\,dr\int_0^\pi \sin\theta\,d\theta\int_0^{2\pi} d\phi(1s)(2s) \times \\ &\int_R^\infty r^2\,dr\int_0^\pi \sin\theta\,d\theta\int_0^{2\pi} d\phi(1s)(2s)\Big\} \end{aligned}$$

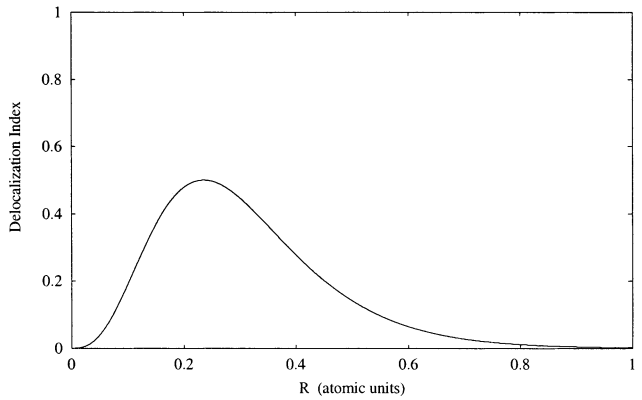

Figure 2. Delocalization index vs radius for C.

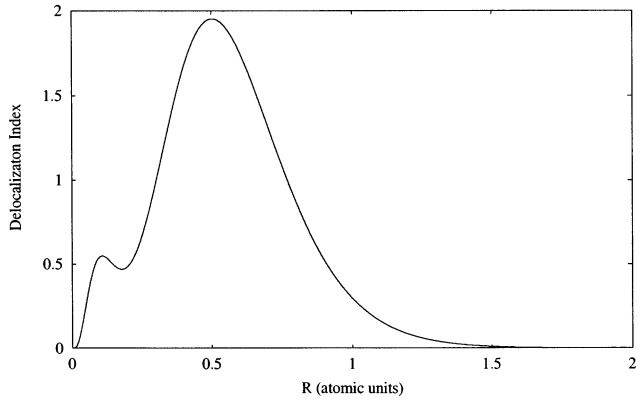

Figure 3. Delocalization index vs radius for Si.

The factor r^2 in each term stems from the volume element dυ expressed in spherical coordinates (r,θ,ϕ). There are no interference terms between the 1s or the 2s orbital and the $2p_{x,y,z}$ orbitals because of the symmetries of the orbitals and the spherical angular integrations. There are no interference terms between the $2p_{x,y,z}$ orbitals due to the presence of harmonics in the $2p_{x,y,z}$ wave functions. In the first three terms of this expression, the value of the second integral is equal to 1 minus the value the first integral because all the orbitals are normalized to 1. In the third term, 3 comes from the presence of the $2p_{x,y,z}$ orbitals having the radial part in common. In the fourth term, the second integral is the negative of the first integral because the 1s and 2s orbitals are orthogonal. The distance from the nucleus, expressed in atomic units given in figures, can be converted to angstroms by 1 au = 0.529177 Å.

The shell structure of the core in carbon is displayed in Figure 2. The core contains only an s orbital. This plot displays a distinct maximum corresponding to a region within the inner shell. The value of 0.5 that the delocalization index has at the maximum is remarkable and related to the number of electrons in the shell. If the value of 0.25 for a single electron, explained in part II, multiples 2, it gives 0.5. The maximum appears at 0.24 atomic units away from the nucleus. If the average radius of the 1*s* orbital is considered as a crude indicator of the orbital size, the value of 0.28 atomic units for the carbon atom is greater than that of 0.24 atomic units corresponding to the position of the distinct maximum.

The structure of the core shells in silicon is displayed in Figure 3. This plot shows both two distinct maxima corresponding to regions within two shells and a distinct minimum corresponding to a region between the shells. The values of the maxima are quite remarkable and related to the number of electrons in each shell. If the value of 0.25 for a single electron multiples 2 and 8, it gives 0.5 and 2, respectively. A minus sign, in front of the interference term between the 1s and the 2s, causes the delocalization index to have a value of a bit less than 2 at the second maximum because the 1s and 2s orbitals are orthogonal. Note, however, the value of the delocalization index of a bit larger than 0.5 at the first maximum and the value of a bit less than 2 that the delocalization index has at the second maximum. The two distinct maxima appear at 0.1 atomic units and 0.48 atomic units away from the nucleus, respectively. The average radius of the 1s orbital of the silicon is 0.12 atomic units, which is greater than the value of 0.1 atomic units corresponding to the position of the first maximum.

Figures 2 and 3 represent an indication of the strengths of the use of the delocalization index to display the shell structure of the electrons in atomic systems.

IV. Delocalization Shell Structure in Atomic Systems

As a quantitative measure of the degree of sharing of an electron between two disjoint regions, the delocalization index is used to display the shell structure of electrons in atoms. The results reported below are based on calculations at the QCISD/6-31++G** level of approximations (including core) using the GAUSSIAN 92[30] suite of programs. The relaxed single particle density matrixes have been used throughout the paper. The atomic overlap integrals are calculated by using the programs ATOMICI[31] and PROAIM.[27] The calculations for atoms beyond the third row of the periodic table of the elements are carried out at the QCISD level of approximations, but the basis sets have been taken from the literature for Kr,[32] Zn,[33] Xe[34], and Rn.[35]

The delocalization indices are calculated for a sequence of the values of *R*. As shown in Figures 4−9, the delocalization indices for the atoms Ne, Ar, Zn, Kr, Xe, and Rn show remarkably well-developed shells. The plots in Figures 4−9 have been generated by the cubic spline routine of the program GNUPLOT.[36] The plots show the distinct maxima and minima corresponding to regions within shells and regions between shells, respectively. The positions of the intershell minima in Figures 4−9 are in good accordance with the positions of the intershell minima reported in the literature.[37,38]

The values of the shell maxima, corresponding to regions within inner shells, are quite remarkable. These values are related to the number of electrons in each shell. The value of 0.25 for an electron is explained in part II. The numbers of electrons in the atomic shells are 2, 8, 18, 32, 18, ..., etc., respectively. If 0.25 is multiplied by the numbers of electrons, it will result in 0.5, 2, 4.5, 8, 4.5, ..., etc., respectively. These numerical values are equal to the values of the maxima corresponding to regions within inner shells, as depicted in Figures 4−9. Physically, the sharing of electrons from each shell does not extend to the regions of the outer shells. This is in agreement with well-known fact that the valence electrons tend to be chemically active. Getting insight into part VI, where a comparison of the delocalization shell structures in atoms constituting molecules to those in atoms is made, supports the conclusion.

The value of *R* at which a distinct maximum appears in the delocalization shell structure is named the radius of the maximum. Note that the shapes of the first two maxima become

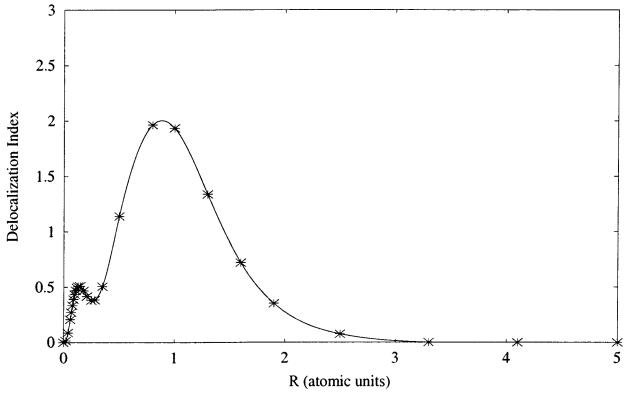

Figure 4. Delocalization index vs radius for Ne.

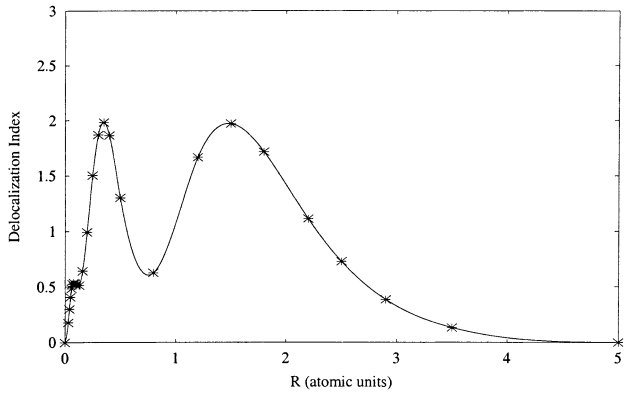

Figure 5. Delocalization index vs radius for Ar.

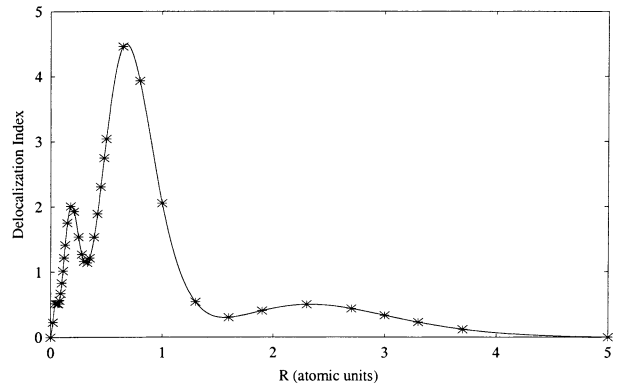

Figure 6. Delocalization index vs radius for Zn.

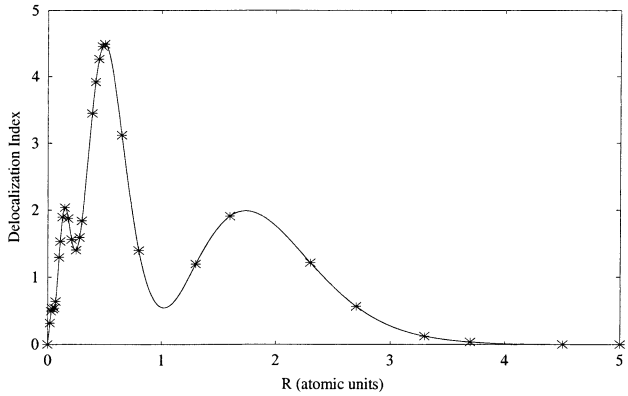

Figure 7. Delocalization index vs radius for Kr.

more like broad shoulders going from the top to the bottom along a column of the periodic table of the elements. This means

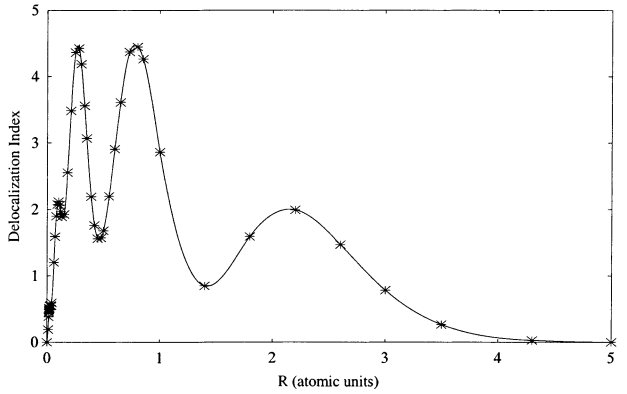

Figure 8. Delocalization index vs radius for Xe.

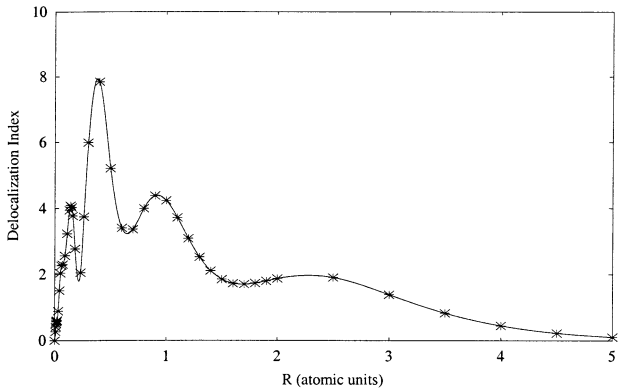

Figure 9. Delocalization index vs radius for Rn.

that the radii of the two maxima, in some cases, do not correspond precisely to a single shell.

V. Contributions of Definite Angular Momenta to the Delocalization Index

In this section, the decomposition of the delocalization index into components of definite angular momenta is carried out. The s-, p-, d-, and f-contributions for Ne, Ar, Zn, Xe, and Au are shown in Figures 10−14, respectively. The delocalization indices for these atoms, plotted by smooth lines, are also given in Figures 10−14. The basis set used to construct the single particle density matrix for Au is taken from the literature.[39]

The values of the maxima of the contributions of definite angular momenta are in agreement with the number of the s ($l = 0$), p ($l = 1$), d ($l = 2$), and f ($l = 3$) electrons in each shell. Thus, if the value of 0.25 for an electron is multiplied by 2, 6, 10, 14, ..., etc., respectively, it will give the values of the maxima of 0.5, 1.5, 2.5, 3.5, ..., etc., respectively. By following the analysis given previously for the total delocalization index, it follows that the sharing of the s ($l = 0$), p ($l = 1$), d ($l = 2$), and f ($l = 3$) electrons from inner shells does not extend to the regions of the outer shells. Interference between the s ($l = 0$), p ($l = 1$), d ($l = 2$), and f ($l = 3$) contributions to the total delocalization index is subastantially restricted to the valence region.

Note that the positions of the maxima of the contributions of definite angular momenta, corresponding to regions within the core shells, appear at almost equal distances from the nuclei in Figures 10−14. The positions of the intershell minima for gold

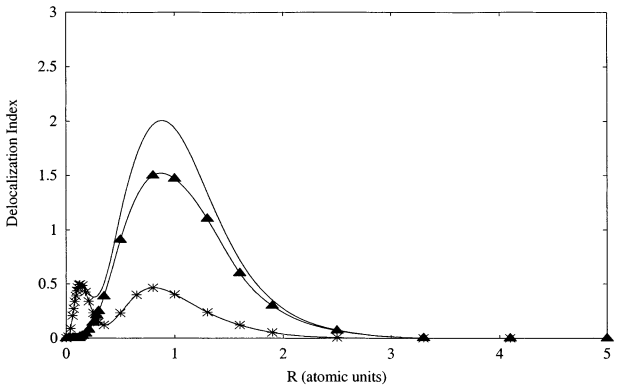

Figure 10. Delocalization index (—), s(*)- and p(▲)-contributions for Ne.

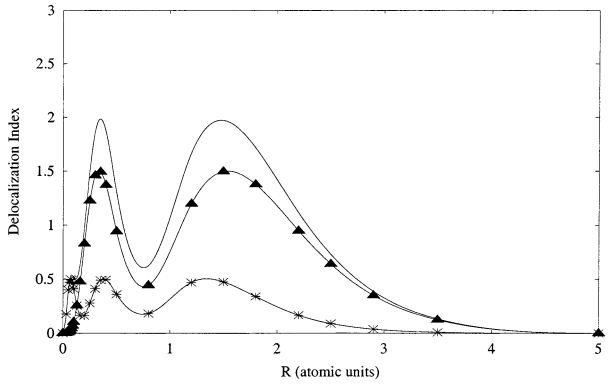

Figure 11. Delocalization index (—), s(*)- and p(▲)-contributions for Ar.

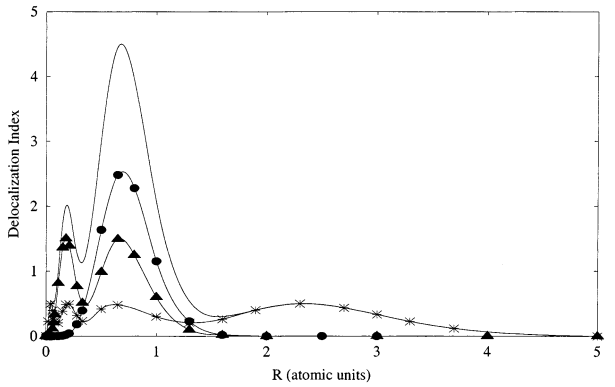

Figure 12. Delocalization index (—), s(*)-, p(▲)-, and d(●)-contributions for Zn.

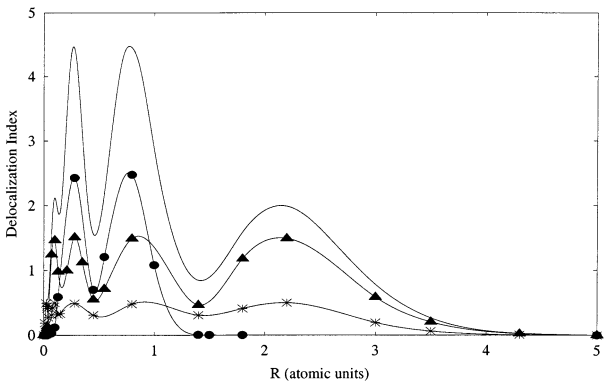

Figure 13. Delocalization index (—), s(*)-, p(▲)-, and d(●)-contributions for Xe.

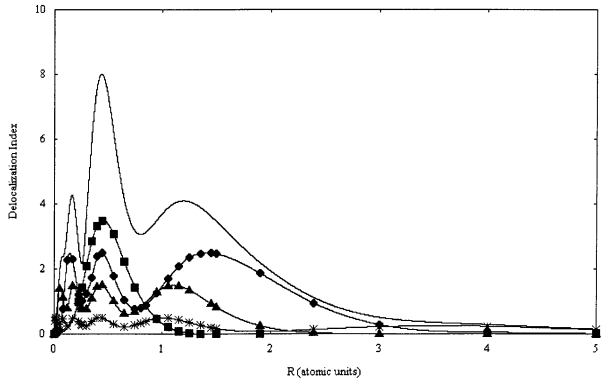

Figure 14. Delocalization index (—), s(*)-, p(▲)-, d(●), and f(■)-contributions for Au.

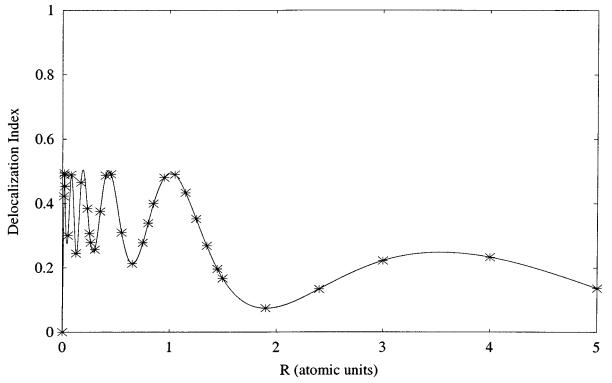

Figure 15. The s-contribution for Au.

given in Figure 14 are in good agreement with those of the radial charge distribution[40] that was constructed for the same basis set.[39] The intershell minima of the contributions of definite angular momenta to the delocalization index determine spatial regions in which the s ($l = 0$), p ($l = 1$), d ($l = 2$), and f ($l = 3$) electrons are essentially localized.

An additional observation with respect to the delocalization shell structure of the gold atom deserves our attention. The delocalization index shows five pronounced maxima, as depicted in Figure 14. On the basis of the assignment of electrons to orbitals, a sixth maximum might be expected to arise from an electron in a 6s orbital.[41] Hence, the s-contribution for Au is given in Figure 15. The sixth maximum of about 0.25 is firmly established.

VI. Electron Delocalization in Molecular Systems

In the previous sections, we developed a detailed picture of the electron delocalization in atomic systems. A natural question to be asked is how the delocalization index is modified when atoms are incorporated into molecules. First, we expect that the delocalization of the core electrons remains essentially unchanged. Second, we expect modifications of delocalization in the valence region.

The results reported below are based on calculations at the QCISD/6-31++G** level of approximations (including core) using the GAUSSIAN 92[30] suite of programs. The optimized molecular geometries are used. The atomic overlap integrals are calculated by using the program ATOMICI.[31]

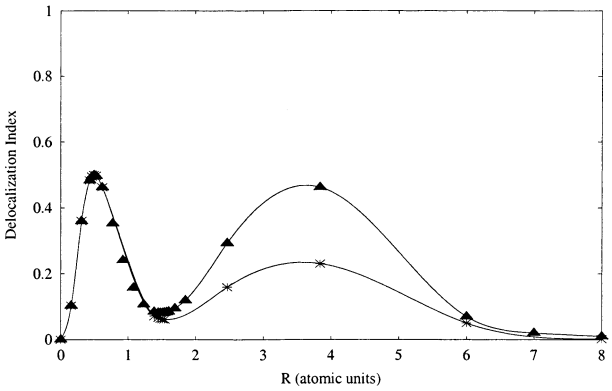

Figure 16. The shell structure for Li(*) and Li(▲) in LiH.

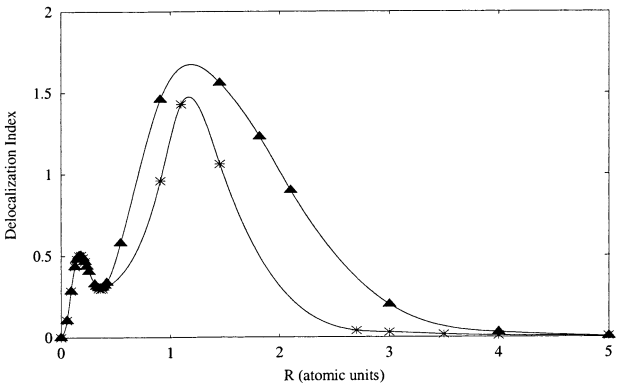

Figure 17. The shell structure for O(*) and O(▲) in H_2O.

The atoms of interest are the heavy atoms Li $^2S_{1/2}$, O $^3P_2$, C $^3P_0$, Si $^3P_0$, N $^4S_{3/2}$, and P $^4S_{3/2}$ in the molecules LiH, H_2O, CH_4, SiH_4, NH_3, and PH_3, respectively. Figures 16−21 give the delocalization shell structures about the heavy atoms in the molecules (symbols ▲) and about the corresponding isolated atoms (symbols *).

The delocalization shell structure about Li in LiH is given in Figure 16. The core shell structure of the electrons in LiH is similar to that in Li. A pronounced maximum of the delocalization index of 0.5 within the inner shell is in agreement with two electrons residing in the core. Hence, the sharing of the core electrons does not extend to the outer shell. As we approach the minimum between the core and the valence region, a difference between the two curves becomes apparent. The impact on the delocalization shell structure in LiH of a donating electron from hydrogen, in comparison to that in Li, is clear in the valence region where the second maximum has the value of a bit less than 0.5. It is interesting to note that the value is not exactly 0.5 which is expected for two electrons forming the Li−H bond. The decomposition of the delocalization index into components of definite angular momenta performed for single atoms in section V showed clearly that interference effects between these components occur and the effects are restricted to the valence region. There is little interference in the shells of the core. The interference effects cause the value of the maximum within valence shell to be a bit less than 0.5. For instance, in the LiH molecule, the explanation of the interference between the 1s and 2s orbitals of Li is possible by means of simulated natural orbitals used. In the expression used to construct the delocalization index as a functon of R in section III, the interference term between the 1s and 2s orbitals of Li is negative because the 1s and 2s orbitals are orthogonal. The negative term lowers the delocalization index in the valence shell. The inclusion of the hydrogen 1s orbital would lead toward further lowering of the delocalization index in the valence region.

The delocalization shell structure about O in H_2O is given in Figure 17. The core shell structure of the electrons in H_2O almost overlaps with that in O indicating that the core electrons have sharing which does not extend to the valence region. A slight difference between the two curves occurs roughly at the intershell minimum. Two donated electrons from the hydrogens forming the bonds in H_2O increase the value of the second maximum of the delocalization index in the valence shell in comparison to that in O.

The delocalization shell structure about C in CH_4 is given in Figure 18. An overlap of the two curves in the inner shells both of C in CH_4 and of the single carbon atom indicates that the core electrons do not share in the valence shell. Four additional electrons from hydrogens increase the value of the second maximum of the delocalization index in the valence region in CH_4 in comparison to that in C.

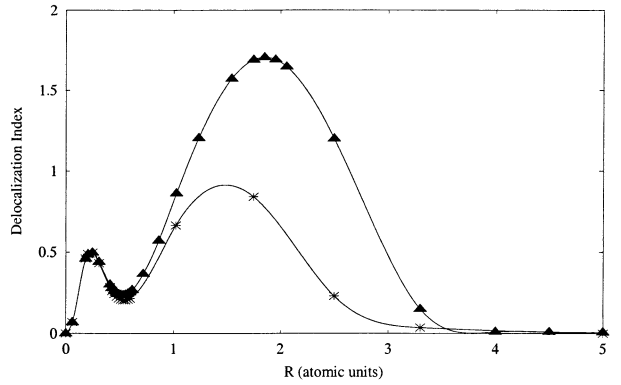

Figure 18. The shell structure for C(*) and C(▲) in CH_4.

The delocalization shell structure about Si in SiH_4 is given in Figure 19. The delocalization of core electrons remains essentially unchanged by bonding four hydrogens to Si and forming SiH_4 in comparison to that in the single Si atom. Following the two curves in the immediate vicinity of the second intershell minimum in Figure 19, the deviation between them becomes recognizable. The addition of four electrons from hydrogens increases the value of the third maximum of the delocalization index in SiH_4 in the valence shell in comparison to that in Si.

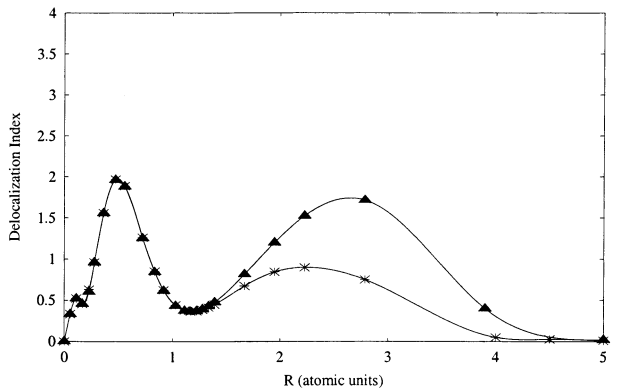

Figure 19. The shell structure for Si(*) and Si(▲) in SiH_4.

The delocalization shell structure about N in NH_3 is given in Figure 20. The inner shell structure in NH_3 almost overlaps with that in N showing that the delocalization of core electrons remains unchanged by bonding three hydrogens to N. The addition of three electrons from hydrogens increases the value of the second maximum of the delocalization index in NH_3 in the valence shell in comparison to that in N.

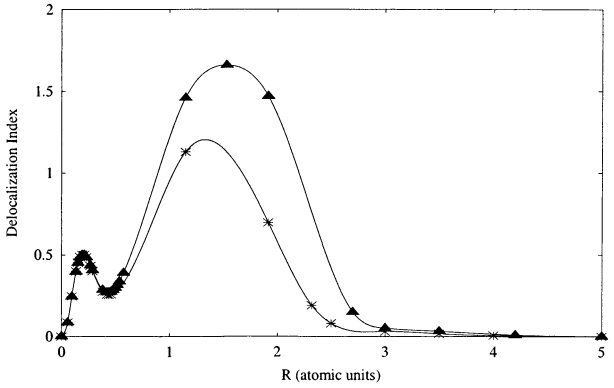

Figure 20. The shell structure for N(*) and N(▲) in NH_3.

The delocalization shell structure about P in PH_3 is given in Figure 21. The delocalization of the core electrons in each shell is pronounced within that shell and unchanged by bonding three hydrogens to P. In the proximity to the minimum between the core and the valence region, the delocalizaton index in PH_3 shows a slight deviation from that in P. The addition of three electrons from hydrogens increases the value of the third maximum of the delocalization index in PH_3 in the valence shell in comparison to that in P.

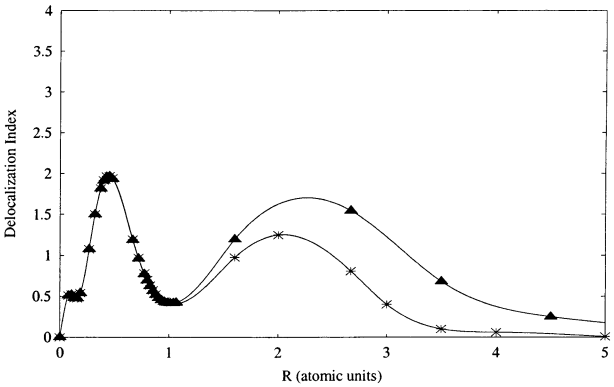

Figure 21. The shell structure for P(*) and P(▲) in PH_3.

The second maxima of the delocalization indices in H_2O, CH_4 and NH_3 have the values of less than 2, a value which is expected for eight electrons in the bonding regions. The third maxima of the delocalization indices in SiH_4 and PH_3 have the values of less than 2, even though eight electrons reside in the bonding regions. Recall that the delocalization indices from spherical volumes of various radii about the heavy atoms O, C, Si, N, and P in the molecules H_2O, CH_4, SiH_4, NH_3, and PH_3, to outside those volumes are calculated, respectively, but a spherical volume about the nuclei is not a satisfactory approximation to an atomic surface in the valence region where bonding between atoms occurs.

The heavy atoms in the molecules have a lowered symmetry. The decomposition of the delocalization index into components of definite angular momenta carried out for single atoms in section V has revealed that interference effects between these components, restricted solely to the valence regions, lower the values of the delocalization indices in the valence regions.

The inclusion of correlation at the QCISD level of approximation in the wave function probably lower the values of the delocalization indices in the valence region.

On one hand, the inspection of the positions of the last maxima, corresponding to regions within the valence shells of the heavy atoms in the molecules, gives the following distances from the nuclei, 3.88 au in LiH, 1.45 au in H_2O, 1.85 au in CH_4, 2.77 au in SiH_4, 1.53 au in NH_3, and 2.65 au in PH_3, respectively. On the other hand, the bond lengths between the heavy atoms and the hydrogens are 3.94 au in LiH, 1.82 au in H_2O, 2.06 au in CH_4, 2.79 au in SiH_4, 1.91 au in NH_3, and 2.67 au in PH_3, respectively, for the optimized geometries. The general trend is that the radii of the maxima within the valence shells around the heavy atoms in the molecules are a bit less than the bond lengths between the heavy atoms and the hydrogens. These deviations are expected because the bond lengths represent the distances between the two centers of bonded nuclei.

The delocalization shell structure in the heavy atoms constituting the molecules shows the bonding regions in Figures 16−21. The broadening of the valence peaks in the molecules with respect to those in the isolated atoms can be viewed as the signature of the bonding.

The core shell structure of the electrons in the molecules is similar to that in the single atoms indicating that the delocalization of the core electrons remains substantially unchanged by incorporating the atoms into the molecules. Hence, our intuition from the beginning of this section is supported.

An additional aspect deserves our attention. The fundamental idea underlying the concept of sharing of an electron[1] in a many electron system is that an electron, as a generalized wave, is delocalized over all the atoms in a molecule. The point-point sharing amplitude $\langle\zeta;\zeta'\rangle$ behaves much like the wave function in the ordinary interpretation of quantum theory. The sharing amplitude is a function of eight (6 spatial + 2 spin) coordinates. For singlet states, this complexity can be simplified somewhat by the fact that the dependence of $\langle\zeta;\zeta'\rangle$ on the spin coordinates is $\delta_{\sigma\sigma'} = \alpha(\sigma)\alpha^*(\sigma') + \beta(\sigma)\beta^*(\sigma')$ so that the amplitude is given by a function of six spatial coordinates. To make the amplitude suitable for the visualization purposes, one coordinate ζ' can be fixed. Call this variable the fixed point. By fixing one point and restricting the system to a singlet, the amplitude $\langle\zeta;\zeta'\rangle$ remains a function of three spatial coordinates. On the basis of the spectral representation of the density matrix,[28] the amplitude may be written, in terms of natural orbitals $\varphi_m(\zeta)$, as

$$\langle\zeta;\zeta'_{\text{fixed}}\rangle = \sum_m \varphi_m(\zeta) a_m$$

where $a_m = \sum_m (N\rho_m)^{1/2}\varphi_m^*(\zeta')$. By writing the natural orbitals as linear combinations of atomic orbitals, the (one fixed point) sharing amplitude may be interpreted in terms of traditional concepts such as hybrid orbitals. The (one fixed point) sharing amplitude has a rich nodal structure which can be used for characterizing chemical bonds in various classes of molecules. The positions of the nodal surfaces are an invariant property of the amplitudes. In some respects the nodal structure is reminiscent of the nodal structure of orbitals. Orbitals sometimes mimic that structure. The idea has been elaborated in a greater detail.[42−45] The present study provides the needed information to locate important fixed points of the sharing amplitudes which can be used in determining the finer details of electron behavior by the sharing amplitudes in the bonding regions of various

classes of molecules. In such fashion, the delocalization index will be directly employed to ferret out connections between this delocalization and the chemical behavior of molecules.

VII. Conclusions

The delocalization index is a quantitative measure of the degree of sharing of an electron between two disjoint volumes in a many electron system.[1] The delocalization index is invariant under transformations of the orbitals in terms of which the wave function is constructed and independent of the sufficiently complete basis set.

The delocalization of an electron in an atom is investigated between two specially chosen volumes of varying extents: an inner spherical volume of radius R centered on the nucleus and the remaining volume. The structure of this delocalization clearly exhibits regions within which electrons are essentially localized and regions between which electrons are greatly delocalized. The delocalization index, as a function of R, shows a remarkable shell-like structure reminiscent of other indicators of shell structure, even in heavy atoms such as radon and gold where by traditional indicators the shell structure is not clear. However, in concept, the present index is quite different from the other measures.

The delocalization shell structure allows us to locate important fixed points of the sharing amplitudes that will be used in the analysis of the sharing of an electron by the sharing amplitudes in bonding regions in various classes of molecules.

Acknowledgment. The author thanks Professor Robert L. Fulton for many constructive ideas.

References and Notes

(1) Fulton, R. L. *J. Phys. Chem.* **1993**, *97*, 7516.
(2) Lewis, G. N. *J. Am. Chem. Soc.* **1916**, *38*, 762.
(3) Lewis, G. N. *Valence and the Structure of Atoms and Molecules; Chemical Catalog Company*; New York, 1923. (a) p 79, (b) p 83, (c) p 67.
(4) Pauling, L. C. *J. Chem. Phys.* **1933**, *1*, 280. Pauling, L. C. *J. Am. Chem. Soc.* **1935**, *57*, 2705.
(5) Coulson, C. A. *Proc. R. Soc.* **1938**−**39**, *A169*, 413.
(6) Cioslowski, J.; Mixon, S. T. *J. Am. Chem. Soc.* **1991**, *113*, 4142.
(7) Wigner, E.; Seitz, F. *Phys. Rev.* **1933**, *43*, 804.
(8) Slater, J. C. *Rev. Mod. Phys.* **1934**, *6*, 209.
(9) Maslen, V. W. *Proc. Phys. Soc. (London)* **1956**, *A69*, 734.
(10) McWeeny, R. *Rev. Mod. Phys.* **1960**, *32*, 335. Bader, R. F. W.; Stephens, M. E. *J. Am. Chem. Soc.* **1975**, *97*, 7391.
(11) Ruedenberg, K. *Rev. Mod. Phys.* **1962**, *34*, 326.
(12) Luken, W. L.; Beratan, D. N. *Theor. Chim. Acta* **1982**, *61*, 265. Luken, W. L. *Croat. Chem. Acta* **1984**, *57*, 1283.
(13) Steiner, E. *The Determination and Interpretation of Molecular Wave Functions*; Cambridge University Press: London, 1976; p 145.
(14) Szabo, A.; Ostlund, N. S. *Modern Quantum Chemistry*; Dover Publications: New York, 1996; p 121.
(15) Becke, A. D.; Edgecombe, K. E. *J. Chem. Phys.* **1990**, *92*, 5397.
(16) Bader, R. F. W.; Essén, H. *J. Chem. Phys.* **1984**, *80*, 1943.
(17) Ángyán, J. G.; Loos, M. *J. Phys. Chem.* **1994**, *98*, 5244−5248.
(18) Fradera, X.; Austen, M. A.; Bader, R. F. W. *J. Phys. Chem. A.* **1999**, *103*, 304−314.
(19) Hunter, G. *Int. J. Quantum Chem.* **1986**, *29*, 197.
(20) Simas, A. M.; Sagar, R. P.; Ku, A. C. T.; Smith, V. H., Jr. *Can. J. Chem.* **1988**, *66*, 1923.
(21) Bader, R. F. W.; MacDougall, P. J.; Lau, C. D. H. *J. Am. Chem. Soc.* **1984**, *106*, 1594.
(22) Sagar, R. P.; Ku, A. C. T.; Smith, V. H., Jr.; Simas, A. M. *J. Chem. Phys.* **1988**, *88*, 4367.
(23) Shi, Z.; Boyd, R. J. *J. Chem. Phys.* **1988**, *88*, 4375.
(24) Sagar, R. P.; Ku, A. C. T.; Smith, V. H., Jr.; Simas, A. M. *Can. J. Chem.* **1988**, *66*, 1005.
(25) Tal, Y.; Bader, R. F. W. *Int. J. Quantum Chem. Quantum Chem. Symp.* **1978**, *12*, 153.
(26) Gillespie, R. J. *Molecular Geometry*; Van Nostrand Reinhold: London, 1972.
(27) Biegler-Konig, F. W.; Bader, R. F.; Tang, T. H. *J. Comput. Chem.* **1982**, *3*, 317.
(28) Löwdin, P. O. *Phys. Rev.* **1955**, *97*, 1474.
(29) Levine, I. N. *Quantum Chemistry*, 4th ed.; Prentice Hall, Inc.: New Jersey, 1991; p 544.
(30) Frisch, M. J.; Trucks, G. W.; Head-Gordon, M.; Gill, P. M. W.; Wong, M. W.; Foresman, J. B.; Johnson, B. G.; Schlegel, H. B.; Robb, M. A.; Replogle, E. S.; Gomperts, R.; Andres, J. L.; Raghavachari, K.; Brinkley, J. S.; Gonzales, C.; Martin, R. L.; Fox, D. J.; Defrees, D. J.; Baker, J.; Stewart, J. J. P.; Pople, J. A. *GAUSSIAN 92*, Revision B; Gaussian, Inc.: Pittsburgh, PA, 1992.
(31) Cioslowski, J.; Nanayakkara, A.; Challocombe, M. *Chem. Phys. Lett.* **1993**, *203*, 317.
(32) Dobbs, K. D.; Hehre, W. J. *J. Comput. Chem.* **1986**, *7*, 359.
(33) Windus, T. L. *J. Chem. Phys.* **1998**, *109*, 1223.
(34) Glendening, E. D.; Feller, D. *J. Phys. Chem.* **1995**, *99*, 3060.
(35) Gropen, O. *J. Comput. Chem.* **1987**, *8*, 982.
(36) Williams, T.; Kelley, C.; et al. *GNUPLOT*, MS−Windows 32 bit, version 3.7, Patchlevel 1, 1999.
(37) Wang, W. P.; Parr, R. G. *Phys. Rev. A* **1977**, *16*, 891.
(38) Boyd, R. J. *J. Chem. Phys.* **1977**, *66*, 356.
(39) Jansen, G.; Hess, B. A. *Chem. Phys. Lett.* **1989**, *160*, 507.
(40) Mitrasinovic, P. M.; Fulton, R. L. A Quantitative Measure of Electron Delocalization in Atomic and Molecular Systems. In *Proceedings of the 2000 International Chemical Congress of Pacific Basin Societies*, Honolulu, 2000; American Chemical Society: Washington, DC, 2000.
(41) Herzberg, G. *Atomic Spectra and Atomic Structure*; Dover Publications: New York, 1994.
(42) Fulton, R. L.; Mixon, S. T. *J. Phys. Chem.* **1995**, *99*, 9768.
(43) Fulton, R. L.; Mixon, S. T. *J. Phys. Chem.* **1993**, *97*, 7530.
(44) Fulton, R. L.; Perhacs, P. *J. Phys. Chem. A* **1998**, *102*, 8988−9000.
(45) Fulton, R. L.; Perhacs, P. *J. Phys. Chem. A* **1998**, *102*, 9001−9020.